

ACTIVE LUBRICATION: FEASIBILITY AND LIMITATIONS ON REDUCING VIBRATION IN ROTATING MACHINERY

Rodrigo Nicoletti

UNICAMP – State University of Campinas, FEM – Department of Mechanical Design, 13083-970, Campinas, Brazil
rodrigo@fem.unicamp.br

Ilmar Ferreira Santos

DTU – Technical University of Denmark, MEK – Department of Mechanical Engineering, 2800, Lyngby, Denmark
ifs@mek.dtu.dk

Abstract: In this work, experimental results show the feasibility of reducing the amplitude of resonance peaks in a rotor-bearing test rig, in the frequency domain, by using active lubricated bearings. The most important consequence of this vibration reduction in rotating machines is the feasibility of increasing their operational range. As a result, one achieves intelligent machines that are more flexible to operate in a fast-changing demand environment. Some limitations of the active lubrication are also discussed based on experimental data, where the response of the servo valves and the supply pressure play an important role: the eigenfrequency of the servo valves establishes the operational frequency range of the active lubrication, whereas the supply pressure establishes the amplitude of vibration reduction achieved with the active lubrication.

Keywords: Vibration Control, Rotordynamics, Tilting-Pad Bearings, Control System, Hydraulics

1. Introduction

Rotating machines like turbogenerators, compressors, turbines, and pumps, are often vital elements in the production process. Therefore, these machines must have not only high performance, but also high availability. In many situations, this availability depends on the adaptation capacity of the machine to fast changing demands. This means that, the operational range of the machine must be flexible.

The dynamic characteristics of a rotating machine strongly depend on the bearings. Once the bearings are designed, the machine has dynamic properties which limit and establish the operational range. The resultant operational range of the machine is not flexible, since the bearings have fixed geometry and, consequently, fixed operational properties. In order to modify the operational properties of the bearing and increase the flexibility of the operational range, one applies the *active lubrication* to the bearings.

When the hydrostatic and the hydrodynamic lubrication are simultaneously combined in a journal bearing, with the aim of reducing wear between machine elements, one refers to the hybrid lubrication, which offers the advantages of both lubrication mechanisms. When part of the hydrostatic pressure is also dynamically modified by means of hydraulic control systems, one refers to the active lubrication. By the association of electronics, control design and hydraulics, the active lubrication simultaneously allows the reduction of wear between rotating and non-rotating parts of the machinery (main purpose of the bearing) and, in addition, the attenuation of rotor vibration. This attenuation of rotor vibration allows the machine to work in a wider operational range, since the operational properties of the bearings can be modified according to the imposed operational conditions (increasing of flexibility).

Active lubrication can also be used in the case of failure of the rotating machine (unbalance, rubbing, blade loss, instability, etc.). By controlling and keeping the shaft vibrations below acceptable limits, the machine is able to continue working until a repair stop, in a suitable moment, can be programmed. Therefore, one eliminates sudden stops and the machine availability is increased.

The first ideas of active lubrication, applied to a tilting-pad bearing, appeared in the work of Santos (1994). Since then, large developments in the modeling has been achieved regarding oil film pressure estimation (Santos and Russo, 1998), oil film temperature estimation (Santos and Nicoletti, 1999), static and dynamic property analyses (Santos and Nicoletti, 2001), and unbalance response control (Nicoletti and Santos, 2003). Few experiment results in the area show that vibration amplitudes can be reduced up to 50% (Santos and Scalabrin, 2003). However, these results only refer to an unbalance response in time domain, in a fixed rotating frequency. The application of active lubrication to other kinds of bearings has also been investigated, namely journal bearings (Wu and Pfeiffer, 1998), hydrostatic bearings (Bently et al., 2000), and multirecess bearings (Santos and Watanabe, 2003).

The objective of this work is to study the feasibility and limitations of active lubrication on the vibration reduction of rotating machines, in frequency domain. A test rig is used, and its frequency response functions (FRFs) are analyzed for the passive (conventional lubrication) and active (active lubrication with proportional controller) cases. A model to estimate the equivalent dynamic coefficients of the active lubrication is presented, and a comparison between numerical and experimental results is performed. A further numerical analysis investigates the limitations of the active lubrication.

2. Test Rig with Actively Lubricated Tilting-Pad Bearing

The actively lubricated bearing under investigation is built by four tilting-pads, in a load-on-pad configuration (Fig. 1). The control action over the rotating shaft is made by injecting oil into the bearing gap through machined bores in the pads (Fig. 2). By coupling hydraulic servo valves to the pads in the vertical and horizontal directions (Fig. 1), the pressure of the injected oil can be controlled. Thus, the hydrodynamic pressure, i.e. the main mechanism of bearing load capacity, can be altered among the different pads, and shaft vibration can be attenuated with help of control techniques.

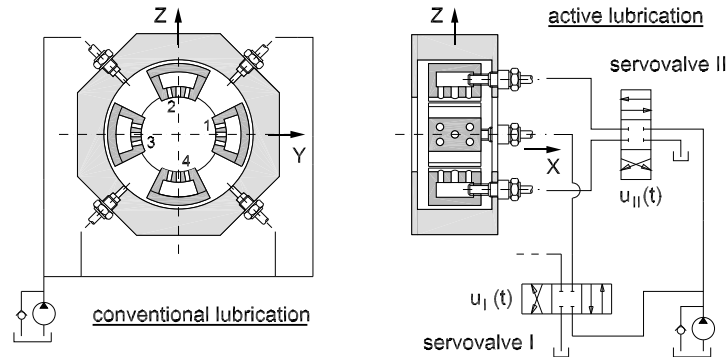


Figure 1: Actively lubricated tilting-pad bearing with injection system.

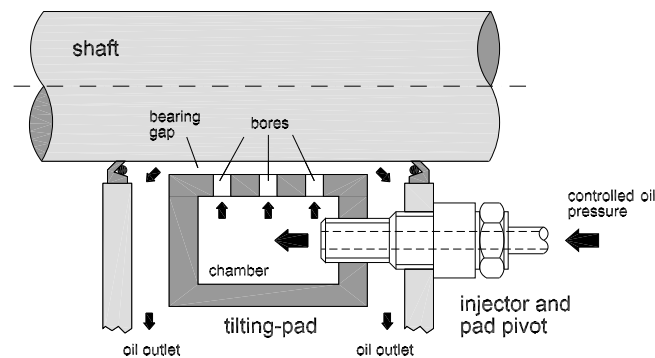


Figure 2: Schematic view of the oil injection system.

It is important to emphasize that conventional lubrication is still the main source of load capacity in this hybrid bearing. In addition, the use of active lubrication in tilting-pad journal bearings has the strong advantage of its negligible cross-coupling effects between orthogonal directions. A secondary advantage of this kind of lubrication is the possibility of cooling the oil film flow, by the injection of oil through the pads (Santos and Nicoletti, 1999, 2001).

Figure 3 shows the test rig of the Department of Mechanical Engineering in the State University of Campinas, where the active tilting-pad bearing is tested. It is composed of a 3 CV electric motor (1), whose rotation is controlled by a frequency converter and connected to a rigid shaft through a flexible joint. The rigid shaft is supported by a self-aligning ball bearing (2) and the active bearing (6). Steel disks (3) are mounted on the shaft, which results to a total weight of 80,9 kg. Eddy current probes (5) are used to measure the shaft displacements in both orthogonal directions, whereas a load cell is used to measure the excitation force.

3. Experimental Results with Proportional Controller

The FRFs of the rotor-active bearing system are obtained by using a chirp signal with period of 2 s and cut-off frequency of 100 Hz. This excitation signal is applied to an electromagnetic shaker, which is connected to the load cell. The load cell is connected to the shaft by a second ball bearing (Fig. 3 (4)). Both force and displacement signals are processed by a signal analyzer.

The control signals to the servo valves are on-line computed by a PC, in a parallel signal processing system. The displacement measurements are filtered and multiplied by the feedback gain (proportional gain), and sent to the servo valves (Fig. 4).

By adopting a controller with proportional gain of 4.8×10^4 V/m, and applying a supply pressure of 8.0 MPa, one obtains the results shown in Fig. 5. The results in Fig. 5 refer to the system response in horizontal direction, for two different rotating frequencies: 15.0 and 30.0 Hz. The FRFs of the system with active lubrication is compared to that of the system with conventional lubrication.

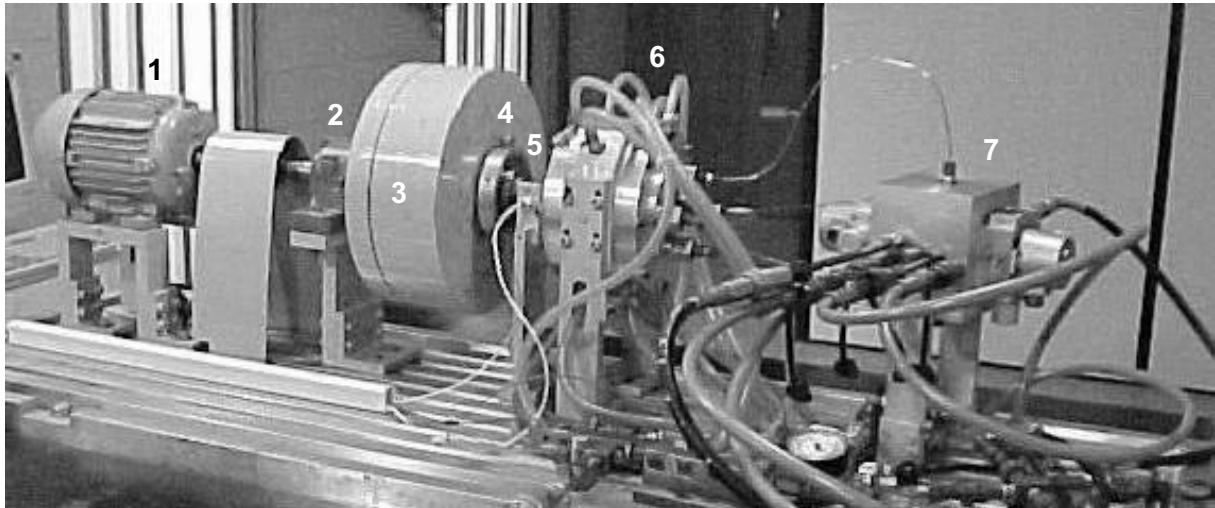


Figure 3: Active Lubricated Bearing Test Rig: 1. electric motor; 2. self-aligning ball bearing; 3. rigid shaft; 4. excitation bearing; 5. eddy current probes; 6. active lubricated tilting-pad bearing; 7. servo valves

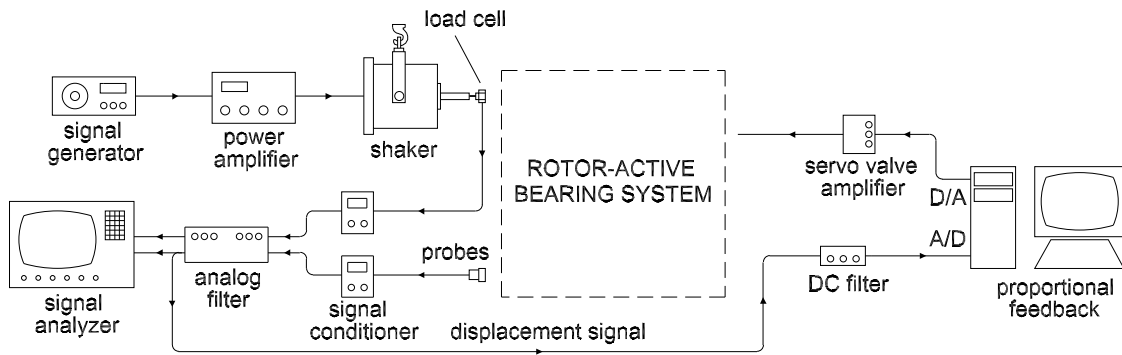


Figure 4: Acquisition and control systems used to obtain the FRFs of the test rig with actively lubricated tilting-pad bearing.

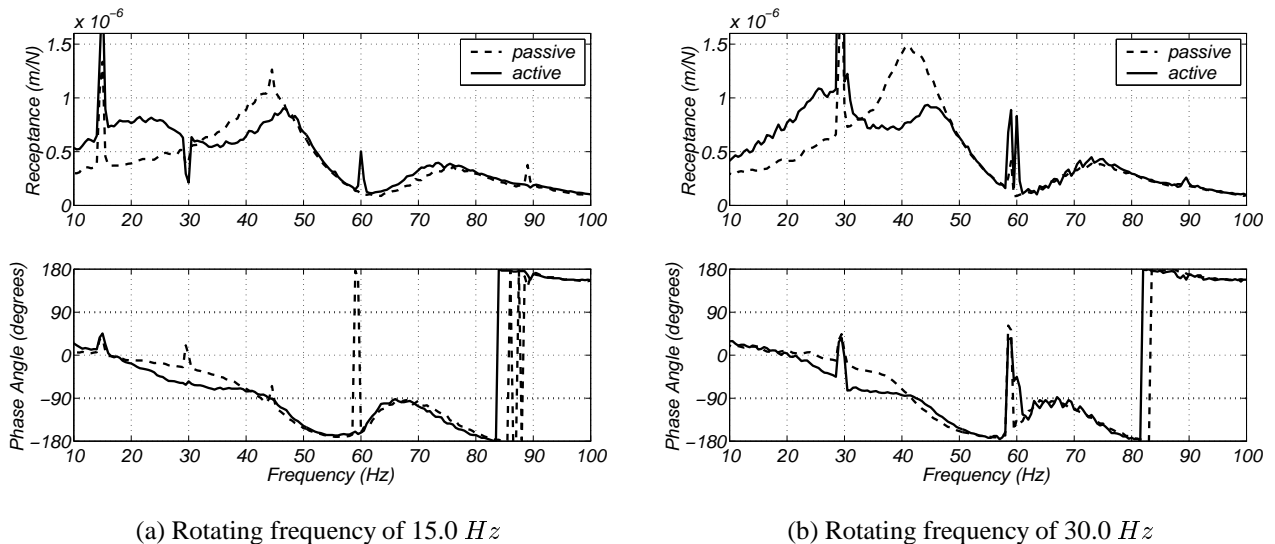


Figure 5: Experimental FRFs of the test rig in the horizontal direction for the passive (conventional lubrication) and active (active lubrication) cases – Proportional control with pressure supply of 8.0 MPa.

As one can see in Fig. 5, the rotor-bearing system with conventional lubrication (passive case) has a resonance peak at the frequency of 42 Hz. When the active system is turned on (active case), the amplitude of the resonance peak has a reduction of near 20% for the rotating frequency of 15.0 Hz, and a reduction of near 30% for the rotating frequency of 30 Hz. The sharp peaks in the FRFs are related to the harmonics of the rotating frequency. Results in the vertical

direction are not presented, because the system has no resonance peaks in this direction, in the frequency range of study (0 to 100 Hz).

The active lubrication managed to reduce the resonance peak of the system, in the frequency domain, by adopting a proportional controller. This means that, in case of need, the system could operate in rotating frequencies near the resonance peak, without presenting excessively high vibration amplitudes due to unbalance. This represents an increase of the operational range of the machine, thus enhancing the machine availability.

4. Mathematical Modeling – Equivalent Dynamic Coefficient Estimation

According to Santos et al. (2001), the hydrodynamic pressure distribution over the four pad surfaces of the active lubricated bearing can be calculated by solving a pair of coupled partial differential equations for each orthogonal direction. For the horizontal direction, the pair of equations is given by Eqs. (1) and (2):

$$\frac{\partial}{\partial \bar{x}} \left(\frac{h_1^3}{\mu} \frac{\partial p_1}{\partial \bar{x}} \right) + \frac{\partial}{\partial \bar{z}} \left(\frac{h_1^3}{\mu} \frac{\partial p_1}{\partial \bar{z}} \right) - \frac{3}{\mu l_o} \sum_{m=1}^{n_o} \mathcal{F}_m [p_1 (1 - C_1) - C_2 p_3] =$$

$$6U \frac{\partial h_1}{\partial \bar{z}} + 12 \frac{\partial h_1}{\partial t} - \frac{3}{\mu l_o} \sum_{m=1}^{n_o} \mathcal{F}_m \left[P_{inj_{st1}} + C_3 \omega_v^2 K_v Y_h \sqrt{\frac{G_{1y}^2 + (\omega G_{2y})^2}{(-\omega^2 + \omega_v^2)^2 + (2 \xi_v \omega_v \omega)^2}} e^{j(\omega t + \phi_y)} \right] \quad (1)$$

$$\frac{\partial}{\partial \bar{x}} \left(\frac{h_3^3}{\mu} \frac{\partial p_3}{\partial \bar{x}} \right) + \frac{\partial}{\partial \bar{z}} \left(\frac{h_3^3}{\mu} \frac{\partial p_3}{\partial \bar{z}} \right) - \frac{3}{\mu l_o} \sum_{m=1}^{n_o} \mathcal{F}_m [p_3 (1 - C_1) - C_2 p_1] =$$

$$6U \frac{\partial h_3}{\partial \bar{z}} + 12 \frac{\partial h_3}{\partial t} - \frac{3}{\mu l_o} \sum_{m=1}^{n_o} \mathcal{F}_m \left[P_{inj_{st3}} + C_3 \omega_v^2 K_v Y_h \sqrt{\frac{G_{1y}^2 + (\omega G_{2y})^2}{(-\omega^2 + \omega_v^2)^2 + (2 \xi_v \omega_v \omega)^2}} e^{j(\omega t + \phi_y)} \right] \quad (2)$$

where p_i is the pressure in the i -th pad; h_i is the oil film thickness in the i -th pad; μ is the oil dynamic viscosity; l_o is the bore length; n_o is the number of bores in a pad; \mathcal{F}_i gives the distribution of bores over the pad surface; U is the shaft surface velocity; t is time; $P_{inj_{st}}$ is the static injection pressure; ω_v is the servo valve eigenfrequency; K_v is the servo valve gain; Y_h is the shaft displacement in the horizontal direction; ξ_v is the servo valve damping factor; and ω is the excitation frequency. The phase angle is given by $\phi_y = \arctg \left[\frac{-G_{1y} 2 \xi_v \omega_v \omega + \omega G_{2y} (\omega_v^2 - \omega^2)}{G_{1y} (\omega_v^2 - \omega^2) + \omega G_{2y} 2 \xi_v \omega_v} \right]$.

For the vertical direction (Z direction), the pair of coupled equations are similar to Eqs. (1) and (2), but referring to pads 2 and 4 instead of pads 1 and 3. These coupled equations are called the modified Reynolds' equations for the active lubrication. Such equations relate the pressure distribution, over each pair of pads arranged in Y and Z directions, with the gains of a generic PD controller by considering the servo valve dynamics. G_{1y} and G_{1z} are the proportional gains, whereas G_{2y} and G_{2z} are the derivative gains. The servo valve dynamics is described by using the constants K_v , ω_v , ξ_v , and K_{PQ} . The coefficients C_1 , C_2 and C_3 are given by:

$$C_1 = \frac{\sum_1^{n_o} \frac{\pi d_o^2}{128 \mu l_o} - K_{PQ}}{\sum_1^{n_o} \frac{\pi d_o^2}{128 \mu l_o} - 2 K_{PQ}} \quad C_2 = \frac{-K_{PQ}}{\sum_1^{n_o} \frac{\pi d_o^2}{128 \mu l_o} - 2 K_{PQ}} \quad C_3 = \frac{1}{\sum_1^{n_o} \frac{\pi d_o^2}{128 \mu l_o} - 2 K_{PQ}} \quad (3)$$

where d_o is the bore diameter; and K_{PQ} is the servo valve linearization factor. The coefficients C_1 and C_2 are the coupling terms between the hydrodynamic pressures over the pair of pads in a given direction. The coefficient C_3 multiplies the term related to the active radial oil injection.

Hence, by a given set of controller gains (G_{1y} , G_{1z} , G_{2y} and G_{2z}), it is possible to calculate the resultant oil film pressure distribution over each pair of pads, considering the effects of the additional radial oil injection.

The dynamic coefficients of the bearing with active lubrication can be estimated by applying a Taylor series and assuming harmonic variation of the oil pressure distribution (Lund and Thomsen, 1978; Ghosh et al., 1989; Hamrock, 1994). Thus, the oil pressure distribution over the i -th pad can be approximated by:

$$p_i = p_i(\bar{x}, \bar{z}, t) = \mathcal{P}_{st_i} + \mathcal{P}_{y_i} \Delta Y_h e^{j\omega t} + \mathcal{P}_{z_i} \Delta Z_h e^{j\omega t} + \mathcal{P}_{\alpha_i} \Delta \alpha_i e^{j\omega t} \quad (4)$$

where:

$$\mathcal{P}_{st_i} = p_i|_{eq} \quad \mathcal{P}_{y_i} = \left. \frac{\partial p_i}{\partial Y_h} \right|_{eq} + j\omega \left. \frac{\partial p_i}{\partial \dot{Y}_h} \right|_{eq} \quad (5)$$

$$\mathcal{P}_{z_i} = \left. \frac{\partial p_i}{\partial Z_h} \right|_{eq} + j\omega \left. \frac{\partial p_i}{\partial \dot{Z}_h} \right|_{eq} \quad \mathcal{P}_{\alpha_i} = \left. \frac{\partial p_i}{\partial \alpha_i} \right|_{eq} + j\omega \left. \frac{\partial p_i}{\partial \dot{\alpha}_i} \right|_{eq}$$

ΔY_h and ΔZ_h are the perturbations on the rotor displacements in horizontal and vertical directions, respectively; ΔA_i is the perturbation on the i -th pad angular displacement; α_i is the i -th pad angular displacement; and eq means the equilibrium position.

The terms \mathcal{P}_{st_i} , \mathcal{P}_{y_i} , \mathcal{P}_{z_i} , and \mathcal{P}_{α_i} are obtained by applying small perturbations to the equilibrium position of the bearing system, and then solving the Reynolds' equation for each pair of pads in the horizontal and vertical directions. Since there are four terms to be calculated for each pad, and the active bearing has four pads, one arrives to a set of sixteen partial equations. By solving numerically this system of equations, one can build for each pad the following matrix:

$$\mathbf{A}_i = \int_{\bar{x}} \int_{\bar{z}} \begin{bmatrix} \mathcal{P}_{y_i} \cos\left(\frac{\bar{z}}{R_s}\right) & \mathcal{P}_{y_i} \sin\left(\frac{\bar{z}}{R_s}\right) & \mathcal{P}_{y_i} (R_s + \Delta s) \sin\left(\frac{\bar{z}}{R_s}\right) \\ \mathcal{P}_{z_i} \cos\left(\frac{\bar{z}}{R_s}\right) & \mathcal{P}_{z_i} \sin\left(\frac{\bar{z}}{R_s}\right) & \mathcal{P}_{z_i} (R_s + \Delta s) \sin\left(\frac{\bar{z}}{R_s}\right) \\ \mathcal{P}_{\alpha_i} \cos\left(\frac{\bar{z}}{R_s}\right) & \mathcal{P}_{\alpha_i} \sin\left(\frac{\bar{z}}{R_s}\right) & \mathcal{P}_{\alpha_i} (R_s + \Delta s) \sin\left(\frac{\bar{z}}{R_s}\right) \end{bmatrix} d\bar{z} d\bar{x} \quad (6)$$

where R_s is the pad inner radius; and Δs is the distance between the pad surface and the pad pivot. Such a matrix is an implicit function of the Sommerfeld number, the excitation frequency (ω), the servo valve dynamics (K_v , ω_v , ξ_v , K_{PQ}), and the control gains of the PD controller (G_{1y} , G_{1z} , G_{2y} , G_{2z}). The stiffness and damping matrices of the i -th rotor-pad subsystem are obtained by the real and imaginary parts of \mathbf{A}_i , as follows:

$$\mathbf{K}_i = \Re(\mathbf{A}_i) \quad (7)$$

$$\mathbf{D}_i = \frac{1}{\omega} \Im(\mathbf{A}_i) \quad (8)$$

By using a transformation matrix \mathbf{T}_i which depends on the position of the pad in the bearing and on the angular displacement of the pad (Allaire et al., 1981), the stiffness and damping coefficients can be calculated in the inertial referential system, for the global rotor-bearing system:

$$\mathbf{K} = \sum_{i=1}^4 \mathbf{T}_i^T \mathbf{K}_i \mathbf{T}_i = \begin{bmatrix} k_{yy} & k_{yz} & k_{y\alpha_1} & k_{y\alpha_2} & k_{y\alpha_3} & k_{y\alpha_4} \\ k_{zy} & k_{zz} & k_{z\alpha_1} & k_{z\alpha_2} & k_{z\alpha_3} & k_{z\alpha_4} \\ k_{\alpha_1 y} & k_{\alpha_1 z} & k_{\alpha_1 \alpha_1} & 0 & 0 & 0 \\ k_{\alpha_2 y} & k_{\alpha_2 z} & 0 & k_{\alpha_2 \alpha_2} & 0 & 0 \\ k_{\alpha_3 y} & k_{\alpha_3 z} & 0 & 0 & k_{\alpha_3 \alpha_3} & 0 \\ k_{\alpha_4 y} & k_{\alpha_4 z} & 0 & 0 & 0 & k_{\alpha_4 \alpha_4} \end{bmatrix} \quad (9)$$

$$\mathbf{D} = \sum_{i=1}^4 \mathbf{T}_i^T \mathbf{D}_i \mathbf{T}_i = \begin{bmatrix} d_{yy} & d_{yz} & d_{y\alpha_1} & d_{y\alpha_2} & d_{y\alpha_3} & d_{y\alpha_4} \\ d_{zy} & d_{zz} & d_{z\alpha_1} & d_{z\alpha_2} & d_{z\alpha_3} & d_{z\alpha_4} \\ d_{\alpha_1 y} & d_{\alpha_1 z} & d_{\alpha_1 \alpha_1} & 0 & 0 & 0 \\ d_{\alpha_2 y} & d_{\alpha_2 z} & 0 & d_{\alpha_2 \alpha_2} & 0 & 0 \\ d_{\alpha_3 y} & d_{\alpha_3 z} & 0 & 0 & d_{\alpha_3 \alpha_3} & 0 \\ d_{\alpha_4 y} & d_{\alpha_4 z} & 0 & 0 & 0 & d_{\alpha_4 \alpha_4} \end{bmatrix} \quad (10)$$

where:

$$\mathbf{T}_i = \begin{bmatrix} \cos(\varphi_i + \alpha_i) & \sin(\varphi_i + \alpha_i) & 0 \\ -\sin(\varphi_i + \alpha_i) & \cos(\varphi_i + \alpha_i) & 0 \\ 0 & 0 & 1 \end{bmatrix} \quad (11)$$

φ_i is the positioning angle of i -th pad inside the bearing; k and d are the equivalent coefficients of stiffness and damping of the oil film. These global rotor-bearing stiffness and damping matrices can be condensed to give the global stiffness and damping coefficients for the horizontal and vertical directions.

5. Numerical Results

The parameters of the bearing and the hydraulic system, used in the numerical analysis, are presented in Tab. 1.

5.1 Comparison Between Numerical and Experimental Results

By setting the derivative gain G_{2y} to zero and using the proportional gain of $G_{1y} = 4.8 \times 10^4 \text{ V/m}$, one calculates the equivalent dynamic coefficients of the active lubrication. Adopting these equivalent dynamic coefficients, one can estimate the theoretical FRFs of the rotor-bearing system. A comparison between the numerical and the experimental FRFs of the system is presented in Fig. 6.

As one can see in Fig. 6, the model of the rotor-bearing system, based on dynamic coefficients of the active lubrication, presents good agreement with the experimental data for both rotating frequencies, specially in the resonance peak. However, the model cannot foresee certain effects, such as the increase of vibration levels in the range between 10 and 30 Hz , or the harmonic components in the FRFs.

Table 1: Parameters of the system in the numerical analysis.

journal radius (R)	24.96	mm	number of orifices per pad (n_o)	5
pad inner radius (R_s)	26.0	mm	assembled bearing gap (h_N)	170.0 μm
pad aperture angle (α_s)	60.0	$^\circ$	oil dynamic viscosity 30°C (μ)	0.043 $\text{N}\cdot\text{s}/\text{m}^2$
pad offset	0.5		servo valve eigenfrequency (ω_v)	320.0 Hz
pad width (W_s)	40.0	mm	servo valve damping factor (ξ_v)	0.48 Hz
distance from surface to pivot (Δs)	19.5	mm	servo valve gain (K_v)	$16.7 \times 10^{-6} \text{ m}^3/\text{s}\cdot\text{V}$
orifice length (l_o) and diameter (d_o)	5.0	mm	servo valve linear factor (K_{PQ})	$1.13 \times 10^{-12} \text{ m}^3/\text{s}\cdot\text{Pa}$

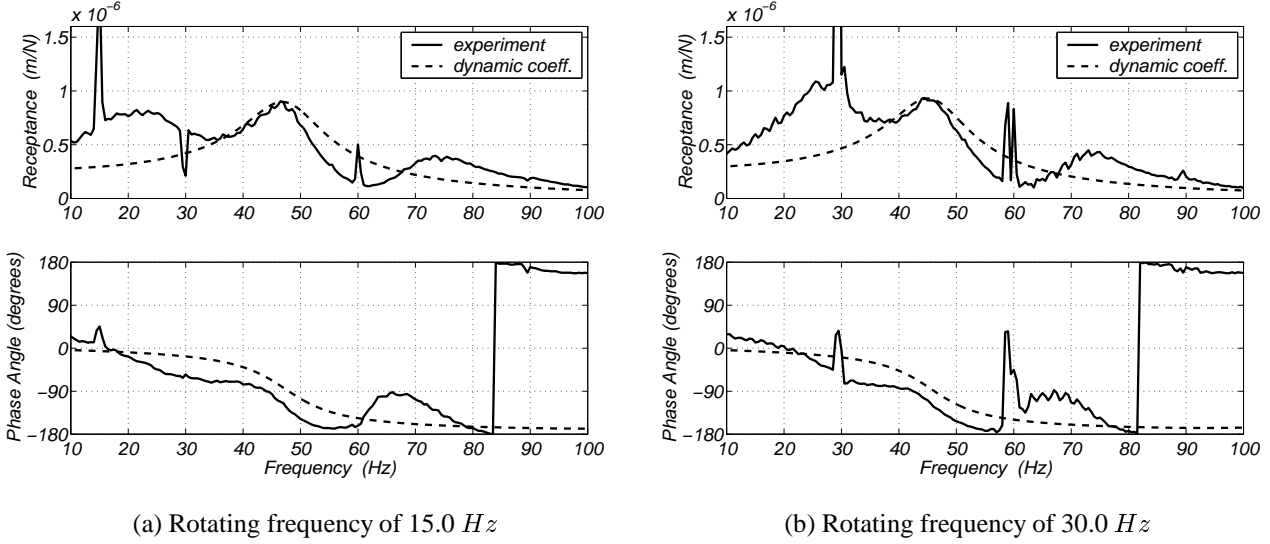


Figure 6: Comparison between experimental and numerical results in the horizontal direction for the active cases – Modeling based on equivalent dynamic coefficients of the active lubrication.

5.2 Global Stiffness and Damping Coefficients

In this part of the work, one investigates the effect of the controller on the global dynamic coefficients of the active lubrication. For that, one has to consider some aspects of the hydraulic system. The operational linear range of servo valves is limited to 5% of its nominal maximum control signal (Schäfer, 1977; Althaus, 1991). Besides, dynamic coefficients are only theoretically valid for infinitesimal displacements. However, according to Lund and Thomsen (1978), dynamic coefficients may be used in practical applications for amplitudes up to 50% of the bearing clearance. With this in mind, the following restrictions of control signal and vibration amplitude were applied to the dynamic coefficients calculations:

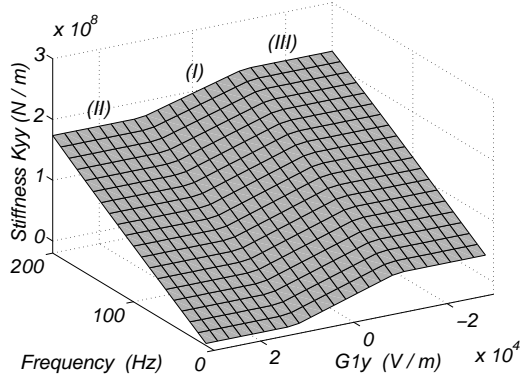
$$\frac{|u_y|}{|Y_h|} = \sqrt{G_{1y}^2 + \omega^2 G_{2y}^2} \leq \frac{0.25}{0.3 h_N} \quad (12)$$

$$\frac{|u_z|}{|Z_h|} = \sqrt{G_{1z}^2 + \omega^2 G_{2z}^2} \leq \frac{0.25}{0.3 h_N}$$

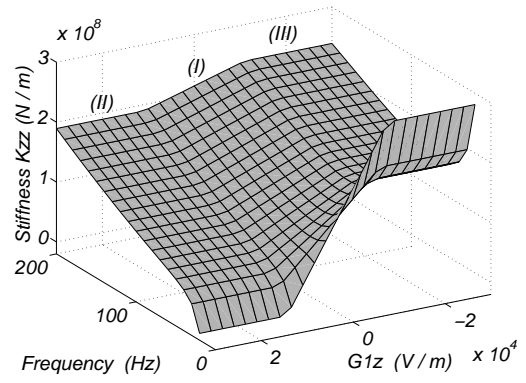
where an amplitude limitation of 30% of the assembled clearance was chosen.

By adopting static pressures of 0.1 MPa in all pads and a supply pressure of 22.0 MPa, and varying the proportional control gains (G_{1y} and G_{1z}), while keeping the derivative gains as zero, one achieves a modification of the stiffness coefficients, while the damping is not much altered. Figure 7 illustrates the behavior of the horizontal and vertical global stiffness coefficients as a function of the proportional gains and rotating frequency. In this figure, for a given control gain, the coefficients K_{yy} and K_{zz} have a standard behavior as function of the rotating frequency, i.e. they increase with the frequency (Someya, 1989). Nevertheless, for a given frequency and varying the control gain, one can detect three different regions in these same figures: region (I) with control gains between $-1.5 \cdot 10^4 \text{ V/m}$ and $+1.5 \cdot 10^4 \text{ V/m}$; region (II) with control gains smaller than $-1.5 \cdot 10^4 \text{ V/m}$; and region (III) with control gains larger than $+1.5 \cdot 10^4 \text{ V/m}$. In region (I), the coefficients K_{yy} and K_{zz} vary linearly as function of the control gains. When the control voltage reaches the limits established by equation (12), the coefficients stop varying and remain constant in the so far achieved values, thus forming regions (II) and (III).

As mentioned previously, the damping coefficients are not much altered by the proportional gains, thus not being presented here. The cross-coupling stiffness coefficients are also not presented since they are negligible, as in the conventional lubrication case.



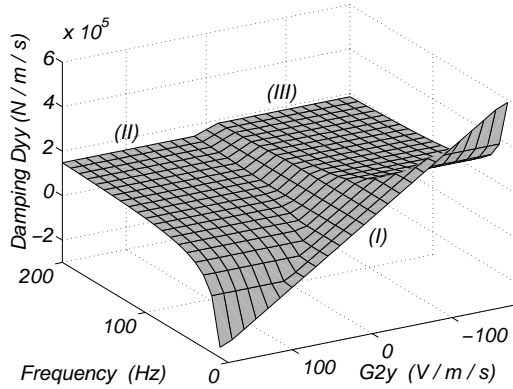
(a) Stiffness in horizontal direction (K_{yy})



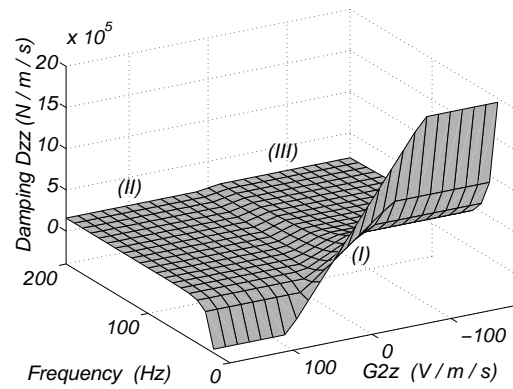
(b) Stiffness in vertical direction (K_{zz})

Figure 7: Stiffness global coefficients of the active lubrication as function of the rotating frequency and proportional gains G_1 .

By setting once again the static pressures to 0.1 MPa, but varying the derivative control gains (G_{2y} and G_{2z}), while keeping proportional gains as zero, one achieves a sensitive modification of the damping coefficients. By this time, the stiffness coefficients are not much altered. Figure 8 illustrates the behavior of the horizontal and vertical main damping coefficients as a function of the derivative gains and rotating frequency.



(a) Damping in horizontal direction (D_{yy})



(b) Damping in vertical direction (D_{zz})

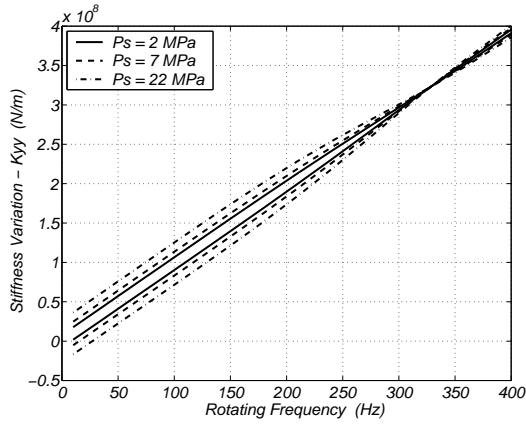
Figure 8: Damping global coefficients of the active lubrication as function of the rotating frequency and derivative gains G_2 .

In Fig. 8, for a given derivative gain, the coefficients D_{yy} and D_{zz} have a standard behavior as function of the rotating frequency, i.e. they decrease with the frequency (Someya, 1989). However, for a given frequency and varying the control gain, one can detect three different regions in Fig. 8 similar to those found in Fig. 7. In region (I), the coefficients D_{yy} and D_{zz} vary linearly as function of the control gains. Nevertheless, such a region narrows with the increase of the rotating frequency. When the control voltage reaches the limits established by equation (12), the coefficients stop varying and remain constant in the so far achieved values, thus forming regions (II) and (III). The narrowing of region (I) is caused by the term ω in equation (12), leading the maximum allowed derivative gain to be a function of the inverse of the frequency ($G_{2y}^{max} = \frac{|u_y|}{|Y_h| \cdot \omega} = \frac{0.25}{0.3 h_N \cdot \omega}$ and $G_{2z}^{max} = \frac{|u_z|}{|Z_h| \cdot \omega} = \frac{0.25}{0.3 h_N \cdot \omega}$).

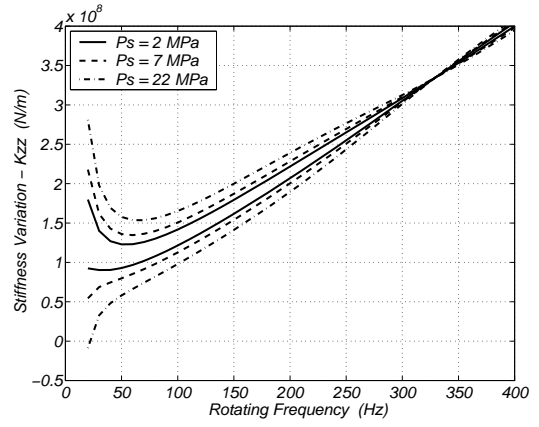
As mentioned previously, the stiffness coefficients are not much altered by the derivative gains, thus not being presented here. The cross-coupling damping coefficients are also not presented since they are negligible, as in the conventional lubrication case.

Figures 7 and 8 show the effect of a PD controller on the dynamic coefficients of a rotor-bearing system with active lubrication. Both stiffness and bearing coefficients can be altered by the active system, resulting in a change of the bearing properties, which is useful to adapt the system to new operational conditions.

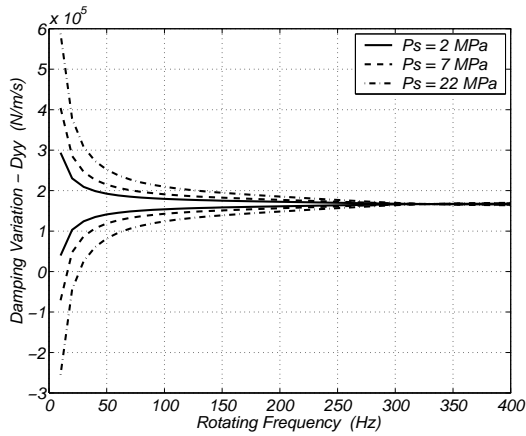
In Fig. 9, the effect of the supply pressure on the variation of the coefficients is presented, where the maximum and minimum achieved values of the coefficients are plotted. One can see that, the higher the supply pressure is, the largest the variation of the coefficients is. This means that, if a larger variation of the coefficients is needed, a higher value of the supply pressure must be adopted, in order to accomplish the desired dynamic characteristics.



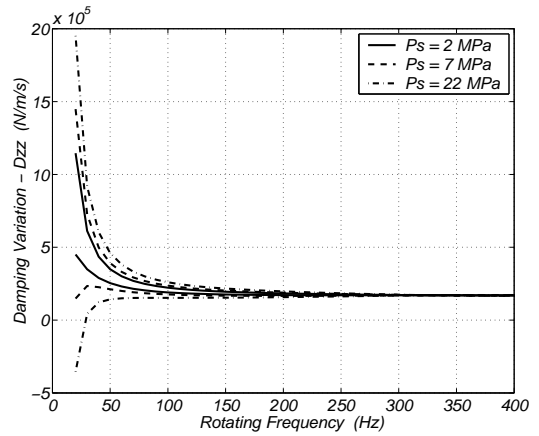
(a) Stiffness in horizontal direction (K_{yy})



(b) Stiffness in vertical direction (K_{zz})



(c) Damping in horizontal direction (D_{yy})



(d) Damping in vertical direction (D_{zz})

Figure 9: Stiffness and damping global coefficients of the active lubrication as function of the rotating frequency and supply pressure.

Another interesting fact shown in Fig. 9 is that the variation of the dynamic coefficients tends to zero when the system operates near the servo valve eigenfrequency (320 Hz). This means that, the efficiency of the active lubrication in changing the dynamic coefficients of the rotor-bearing system depends on the servo valve dynamics. The faster the servo valve responds the control signals, the larger the operational range of the active lubrication is.

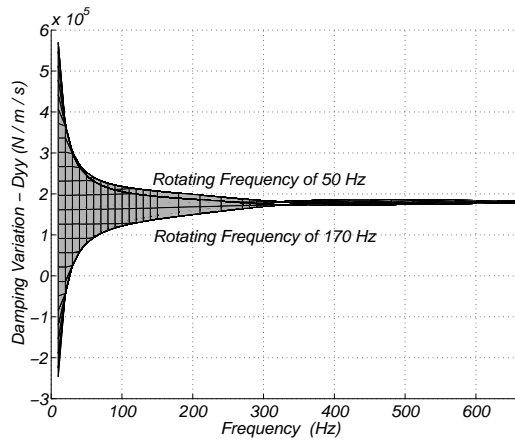
Figures 10 and 11 present the variation of the dynamic coefficients as function of the excitation frequency and the derivative gain (G_2), for the horizontal and vertical directions respectively. In these figures, one can see that near the servo valve eigenfrequency (320 Hz), the system presents low variations of damping and large variations of stiffness. This means that, exciting the system near the servo valve eigenfrequency results in the increase of stiffness without any changing in the damping of the system, which is an undesirable dynamic situation for the machine. In other words, excitations near the servo valve eigenfrequency must be avoided when the active lubrication is in use.

6. Conclusion

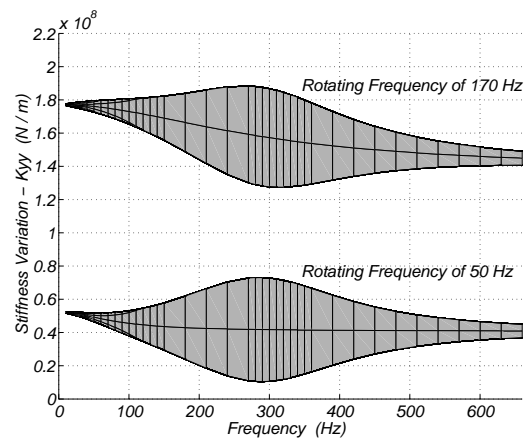
In this work, the concept of active lubrication is studied both numerically and experimentally. Experimental results in a test rig, using a proportional controller, showed the feasibility of reducing the resonance peak amplitude up to 30% of its original value. By reducing the resonance peak amplitude, it is possible to operate the machine in a wider range of frequencies than that of a machine with conventional lubrication.

A mathematical model is presented, whose objective is the estimation of the equivalent dynamic coefficients of the active lubrication. By adopting this model and calculating the coefficients, one obtains the theoretical FRFs of the system. Good agreement is achieved in the comparison between numerical and experimental results.

Further numerical analyses in the influence of the active lubrication on the dynamic coefficients show that, these coefficients can be significantly altered by varying both the proportional and the derivative gains of a PD controller. In addition, the maximum and minimum achieved values of the coefficients depend on the supply pressure level. The higher the supply pressure is, the larger the variation of the coefficients is. However, near the servo valve eigenfrequency, the variation of the coefficients is almost null. Therefore, *the supply pressure and the servo valve eigenfrequency are limiting*

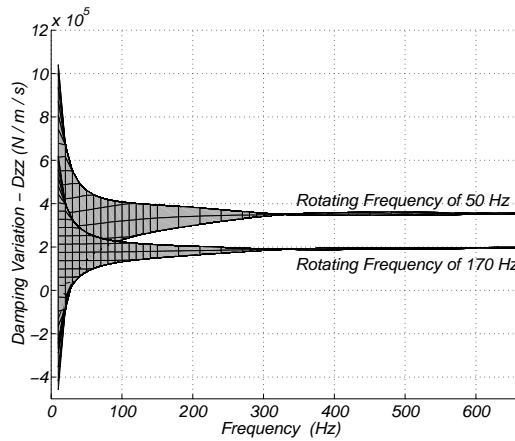


(a) Damping in horizontal direction (D_{yy})

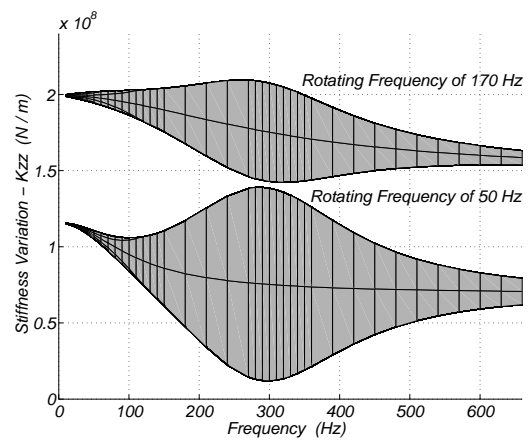


(b) Stiffness in horizontal direction (K_{yy})

Figure 10: Stiffness and damping global coefficients of the active lubrication as function of the harmonic excitation frequency and the derivative gain G_{2y} in the horizontal direction – Rotating frequencies of 50 and 170 Hz.



(a) Damping in vertical direction (D_{zz})



(b) Stiffness in vertical direction (K_{zz})

Figure 11: Stiffness and damping global coefficients of the active lubrication as function of the harmonic excitation frequency and the derivative gain G_{2z} in the vertical direction – Rotating frequencies of 50 and 170 Hz.

factors of the active lubrication, and must be taken into account for the proper functioning of the active system.

A disadvantage of the active lubrication appears when the excitation frequency is near the servo valve eigenfrequency. In this situation, the system presents higher stiffness values, while the damping remains constant, leading the system to undesirable dynamic conditions. Hence, the use of active lubrication must be avoided when the excitation frequency is near the servo valve eigenfrequency.

7. Acknowledgment

The Brazilian research foundation FAPESP – Fundação de Amparo à Pesquisa do Estado de São Paulo is gratefully acknowledged by the support given to this project.

8. References

- Allaire, P. E., Parsell, J. A., and Barret, L. E., 1981, "A Pad Perturbation Method for the Dynamic Coefficients of Tilting Pad Journal Bearings", *Wear*, Vol. 72, pp. 29-44.
- Althaus, J., 1991, "Eine aktive hydraulische Lagerung für Rotorsysteme", *Fortschritt-Berichte VDI*, Series 11, No. 154, VDI-Verlag GmbH, Düsseldorf, 150p.
- Bently, D. E., Grant, J. W., and Hanifan, P. C., 2000, "Active Controlled Hydrostatic Bearings for a New Generation of Machines", *Trans. of ASME - J. of Engineering for Gas Turbines and Power* (pre-print 2000-GT-354).
- Ghosh, M. K., Guha, S. K., and Majumdar, B. C., 1989, "Rotordynamic Coefficients of Multirecess Hybrid Journal Bearings - Part I", *Wear*, Vol. 129, pp. 245-259.
- Hamrock, B. J., 1994, "Fundamentals of Fluid Film Lubrication", *Mechanical Engineering Series*, McGraw-Hill Book Co., New York, 750p.

- Lund, J. W., and Thomsen, K. K., 1978, "A Calculation Method and Data for the Dynamic Coefficients of Oil-Lubricated Journal Bearings", *Topics in Fluid Film Bearing and Rotor Bearing System Design and Optimization*, ASME, pp. 1-28.
- Nicoletti, R., and Santos, I. F., 2003, "Linear and Non-Linear Control Techniques Applied to Actively Lubricated Journal Bearings", *J. of Sound and Vibration*, Vol. 260, No. 5, pp. 927-947.
- Santos, I. F., 1994, "Design and Evaluation of Two Types of Active Tilting-Pad Journal Bearings", *Proceedings of IUTAM Symposium on Active Control of Vibration*, Bath, England, pp. 79-87.
- Santos, I. F., and Nicoletti, R., 1999, "THD Analysis in Tilting-Pad Journal Bearings Using Multiple Orifice Hybrid Lubrication", *Trans. of ASME - J. of Tribology*, Vol. 121, No. 4, pp. 892-900.
- Santos, I. F., and Nicoletti, R., 2001, "Influence of Orifice Distribution on the Thermal and Static Properties of Hybridly Lubricated Bearings", *Int. J. of Solids and Structures*, Vol. 38, No. 10-13, pp. 2069-2081.
- Santos, I. F., and Russo, F. H., 1998, "Tilting-Pad Journal Bearings with Electronic Radial Oil Injection", *Trans. of ASME - J. of Tribology*, Vol. 120, No. 3, pp. 583-594.
- Santos, I. F., and Scalabrin, A., 2003, "Control System Design for Active Lubrication with Theoretical and Experimental Examples", *Trans. of ASME - J. of Engineering for Gas Turbines and Power*, Vol. 125, No. 1, pp. 75-80.
- Santos, I. F., Scalabrin, A., and Nicoletti, R., 2001, "Ein Beitrag zur aktiven Schmierungstheorie", *Proceedings of SIRM, Schwingungen in rotierenden Maschinen V*, Viena, Austria, Vol. 5, pp. 21-30.
- Santos, I. F., and Watanabe, F. Y., 2003, "Feasibility of Influencing the Dynamic Fluid Film Coefficients of a Multirecess Journal Bearing by Means of Active Hybrid Lubrication", *J. of the Brazilian Society of Mechanical Sciences and Engineering*, Vol. 15, No. 2, pp.154-163.
- Schäfer, K. D., 1977, "Elektrohydraulische regelsysteme", *MOOG Bulletin D*, Vol. 1, No. 180, WA 2000 N.
- Someya, T., 1989, "Journal Bearing Data Book", Springer Verlag, Berlin, 320p.
- Wu, W., and Pfeiffer, F., 1998, "Active Vibration Damping for Rotors by a Controllable Oil-Film Bearing", *Proceedings of the 5th IFToMM Int. Conf. on Rotor Dynamics*, Darmstadt, Germany, pp. 431-443.